Journal of Alloys and Compounds 509 (2011) 6350–6353

Contents lists available at ScienceDirect

Journal of Alloys and Compounds

journal homepage: www.elsevier.com/locate/jallcom

Superconducting property and Fe valence state of FeSe thick films grown from high temperature solution

Xiaoding Qi [a,*], Jiun-Yi Wang [a], Jui-Chao Kuo [a], Karen A. Yates [b], Lesley F. Cohen [b]

[a] Department of Materials Science and Engineering, National Cheng Kung University, Tainan City 70101, Taiwan
[b] Department of Physics, Imperial College, London SW7 2BP, UK

ARTICLE INFO

Article history:
Received 18 July 2010
Received in revised form
26 December 2010
Accepted 7 March 2011
Available online 12 March 2011

Keywords:
FeSe
Superconductor
Thick film

ABSTRACT

Thick FeSe films (1–2 μm) were grown from high temperature solution with SeSn as the flux. Electron backscatter diffraction confirmed the films of tetragonal β phase with high crystallinity. Superconducting transition was observed by magnetic measurements, with the onset T_c of 6.1 K for the as-grown films and rising to 6.9 K after post-growth annealing at 400 °C, which was still 1.5 K lower than the sintered powder samples. X-ray photoelectron spectroscopy showed that the Fe $2p_{3/2}$ binding energy in the FeSe compound was composed of two peaks at 707.8 eV and 706.6 eV, respectively. The former was close to the value of Fe in polarized ionic bonds, while the later had the typical value in metallic bondings. The ratio of the two bondings was 1.56 and 1.94 for the films and sintered powders, respectively. The critical temperature may have some correlation with the ratio of the two bondings. A lower average Fe valence was probably the cause for the lower T_c observed in thick films.

1. Introduction

The discovery of Fe-based superconductors in the early 2008 ended the monopoly of cuprates in the unconventional high-T_c superconductivity, in which the Cooper pairs were thought to be mediated via spin fluctuations rather than phonons. Initial results show some similarities as well as differences between the two and in many respects, Fe-based superconductors sit between the cuprates and MgB_2 [1]. In the crystal structures of both cuprates and Fe compounds, there exist Cu or Fe layers that are crucial to superconductivity. However, for the Fe compounds the spacer between the two adjacent Fe layers can be absent, leading to a very simple compound, FeSe [2]. Unlike Fe-pnictides, whose parent compounds are magnetic, FeSe shows Pauli paramagnetism above T_c [2]. The magnetic order occurs after doping of over 50 at.% Te and the T_c is raised up to 15 K just before this concentration [3,4]. The superconductivity in FeSe is sensitive to the Ti, V, Cr and Cu doping, which disappears completely at the dopant concentration of up to 3 at.% [5,6]. Doping of other elements, such as Al, Ga, Ba, Sm, Mn, Ni, Co, etc., only results in small changes of T_c [6,7]. On the other hand, T_c can be raised significantly to 27 K by applying high pressure [8]. Compared to Fe-pnictides, FeSe is much less understood and more studies are needed.

There are at least three compounds of the composition around the atomic ratio 1:1 in the Fe–Se binary system [9], i.e. the Fe-rich tetragonal β phase ($FeSe_{1-x}$), the Se-rich hexagonal δ phase ($FeSe_{1+x}$), and the stoichiometric compound, Fe_7Se_8. The superconductivity is only found in the β phase (also called as α phase in some papers) [2]. However, the synthesis of a pure β phase by the conventional solid state sintering seems to be difficult. Most samples shown in recent publications contained some amounts of δ phase and/or Fe_7Se_8, as well as the traces of metallic α-Fe and iron oxides [2,7,10]. In this paper, a novel liquid phase processing method was used to grow the thick films of a pure β-phase, with a quality similar to single crystal. However, the T_c of the thick films was lower than the sintered powder samples. A number of experiments were therefore carried out to identify the cause and the main findings are presented in this paper.

2. Experimental

FeSe films were grown from high-temperature solution with SeSn as the flux. This was a process similar to single crystal growth from liquid phase. First, FeSe and SeSn were prepared separately from the metallic powders of Fe, Se and Sn by solid state reaction, and then the two were mixed according to the ratio 90% FeSe + 10% SeSn by grinding in an agate mortar. For a better mixing and also avoiding absorption of ambient moisture, water-insoluble toluene was added to the mixture during grinding. The dried powder mixture was pressed into the disks of thickness 2–5 mm and diameter 10 mm. A charge of about 5 g was placed in an alumina boat and melted at 910 °C under the flowing Ar + 3%H_2 atmosphere to form a liquid, according to the FeSe–SeSn phase diagram [9]. Upon cooling down slowly to 800 °C, FeSe was precipitated on the (0 0 1) $LaAlO_3$ (LAO) substrate, as well as on the Al_2O_3 boat surface. The furnace was then quickly cooled to room temperature at 600 °C/h. The details about the growth process and experimental setup were described elsewhere [10].

* Corresponding author. Tel.: +886 6 2008060.
E-mail address: xqi045@mail.ncku.edu.tw (X. Qi).

0925-8388/$ – see front matter © 2011 Elsevier B.V. All rights reserved.
doi:10.1016/j.jallcom.2011.03.054

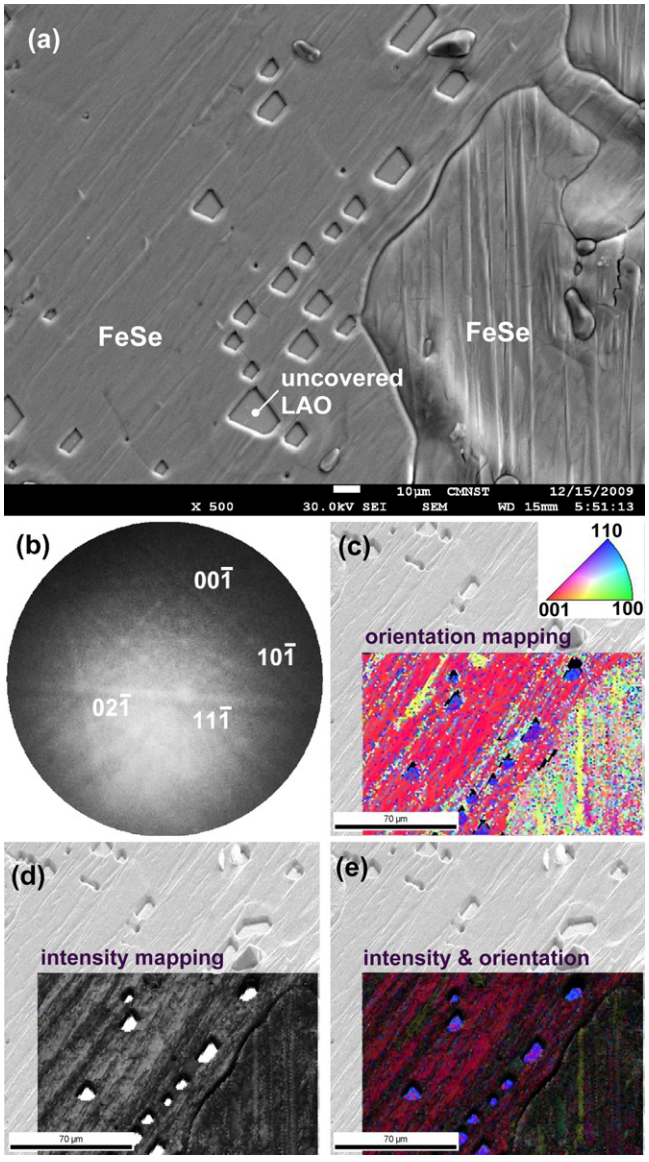

Fig. 1. (a) SEM image over an area of 250 μm × 200 μm, (b) EBSD pattern, which can be indexed with the space group *P*4/*nmm* and the lattice parameters of β-FeSe, (c) EBSD orientation mapping, (d) EBSD intensity mapping, and (e) combined signal of intensity and orientation. In EBSD the sample was tilted about 70° for recording diffraction patterns.

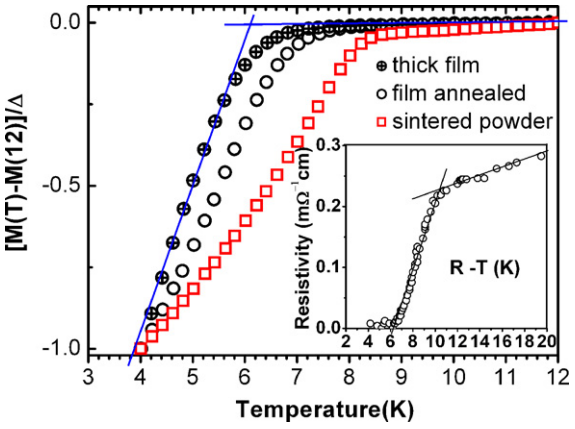

Fig. 2. *M*–*T* curves of the as-grown film, the film annealed at 400 °C, and sintered powder. The *y*-axis is normalized against the magnetization drop from 12 K to 4 K, i.e. $\Delta = M(12) - M(4)$. *Inset*: *R*–*T* curve measured on the sintered powder pellet.

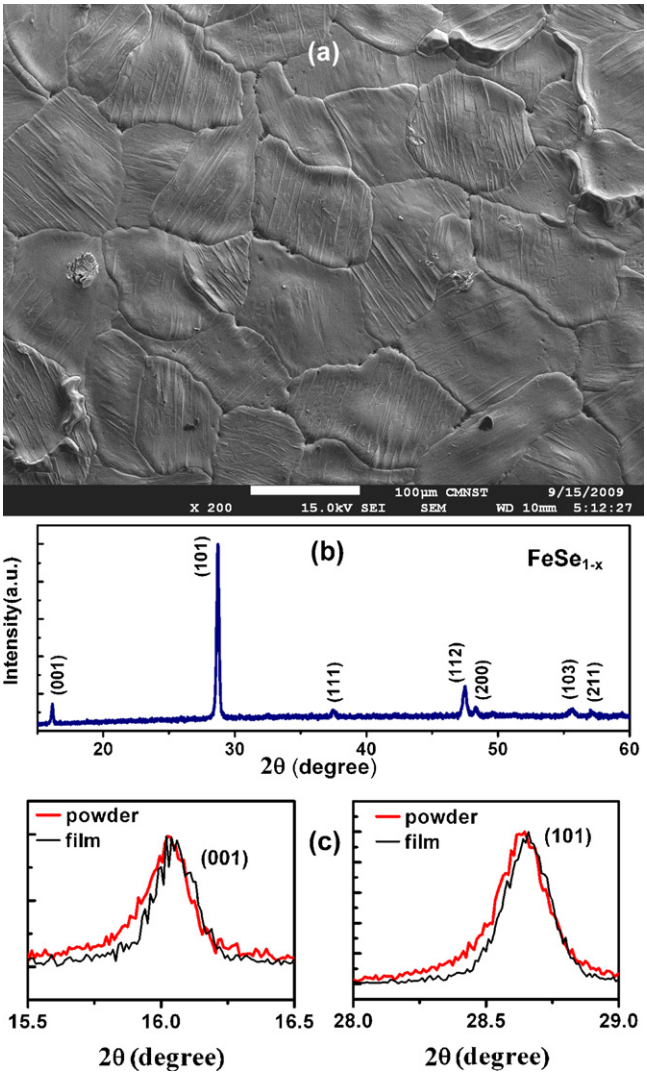

Fig. 3. (a) SEM of a thick film grown on polycrystalline alumina surface, (b) XRD pattern of such a film, showing preferred orientation of (1 0 1), and (c) comparison of XRD peaks for the film and sintered powder.

3. Results and discussion

Shown in Fig. 1(a) is the scanning electron microscopy (SEM) image of such a film, which had the thickness of about 1.5 μm, as measured by a stylus profilometer scanning across the junctions between the film and uncovered substrate. Compositional analysis by the energy dispersive X-ray spectroscopy (EDS) showed that the thick films had the Fe:Se ratio approximately equal to 1 within the experiment error. The thick films were confirmed to have the superconducting β-phase by the electron backscatter diffraction (EBSD), whose pattern matched with the tetragonal *P*4/*nmm* space group and the FeSe lattice parameters $a = b = 3.765$, $c = 5.518$ Å (PDF#85-0735), as shown in Fig. 1(b). For the well wetted part of the substrate surface, the thick film seemed to grow epitaxially on the (0 0 1) LAO (pseudo-cubic $a \approx 3.79$ Å), as shown in the EBSD orientation mapping in Fig. 1(c). For the film formed from excess liquid (e.g. right side of Fig. 1(a)), other orientations were obtained. Nevertheless, all areas of the film exhibited a good crystallinity and uniform composition, as shown by the EBSD intensity mapping and the combined intensity and orientation mapping in Fig. 1(d) and (e), respectively. Although the FeSe–SeSn phase diagram showed some solid solubility of Sn in FeSe [9], EDS failed to find any Sn trace in the films within its sensitivity of 0.1 at.%. Residual Sn was later found to be in

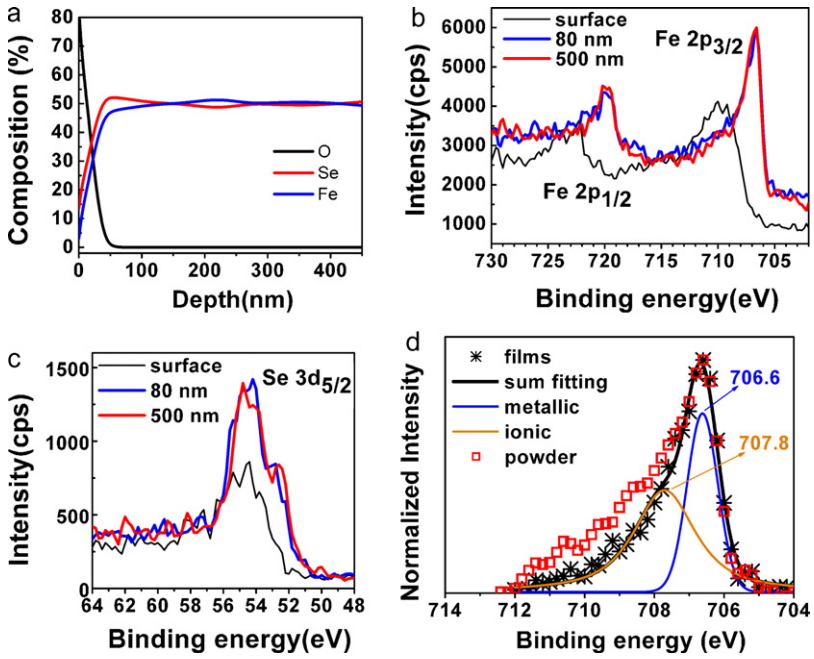

Fig. 4. (a) XPS depth profile of composition for a film kept in desiccator for 6 months, (b) Fe 2p binding energy measured at the surface and at the depths of 80 nm and 500 nm below the surface, (c) Se $3d_{5/2}$ binding energy measured at different depths, and (d) comparison of the Fe $2p_{3/2}$ peak for the film and sintered powder, the deconvolution was done for both samples, but only the fitting for film is shown here to avoid overcrowding.

the order of 4 ppm by the inductively coupled plasma mass spectrometry (ICP-MS), equipped with an excimer laser for the ablation of solid source. ICP-MS also gave a Fe:Se ratio of 1.03:1, confirming the earlier EDS result. The absence of Sn in thick films was ascribed to its large evaporation rate at high temperature [10].

Magnetization vs. temperature (M–T) measurements was carried out by the SQUID magnetometry. Shown in Fig. 2 are the M–T curves recorded in the applied field of 10 Oe upon heating up. For easy comparison of different samples, the y-axis was normalized against the magnetization drop from 12 K to 4 K. The as-grown FeSe films showed a superconducting transition at the onset T_c of 6.1 K, which was taken at the intersection point of the two extrapolated lines. Compared to the sintered powder sample, there was 2.3 K reduction of T_c for the thick film. To clarify if the Sn contamination was responsible, 5 at.% doped FeSe powder samples were sintered, which showed little change of T_c [10]. To shed some light on the transition width from the onset to zero-resistance state, the resistivity vs. temperature measurement was carried out by the 4-point method, which showed a transition region of 2.8 K (inset of Fig. 2).

To see the strain effect, the thick films were subjected to a post-growth annealing at 400 °C for 24 h. The T_c of the annealed films was only slightly increased, as compared in Fig. 2, indicating that strain was not the main cause for the T_c depression. Recently, the thickness and orientation dependences of T_c were reported for the epitaxial FeSe films grown at 320–500 °C by pulsed laser deposition [11]. The (0 0 1) textured films showed a significantly depressed T_c when their thickness was less than 1.0 μm, while the (1 0 1) textured films exhibited only small T_c variation with thickness [11]. As mentioned earlier, the film thickness in this study was about 1.5 μm and therefore should not be relevant. To confirm this, we measured the FeSe films precipitated on the Al_2O_3 boat surface from the same high temperature liquid. The SEM image of such a sample is shown in Fig. 3(a), which reveals that the film was composed of large grains of over 100 μm in diameter. X-ray diffraction (XRD) showed that the film had a preferred (1 0 1) orientation, as shown in Fig. 3(b). The measurements on such samples showed same T_c drops as the films on (0 0 1) LAO. The XRD peaks of the thick film and sintered powder are compared in Fig. 3(c), which shows little shift of peak position but a narrower width for the thick film, reflecting its better crystallinity. Therefore, structure distortion may also be ruled out for the T_c depression.

X-ray photoelectron spectroscopy (XPS) was carried out to check the valence state of Fe and Se. The XPS data were collected with the monochromatic MgKα (1253.6 eV) radiation by a JEOL 9010MX system. The measured binding energies were calibrated against the C 1s peak (284.6 eV) of the residual carbon absorbed on the surface from the ambient atmosphere. It was observed that there was a slow diffusion of oxygen into the FeSe thick films. Fig. 4(a) shows the depth profile of composition for a film kept in a desiccator for 6 months. Oxygen diffused into the film up to a depth of 50 nm. XPS on the surface layer showed that the Fe $2p_{3/2}$ binding energy was 709.4 eV (Fig. 4(b)), the same as the value of Fe^{2+} in FeO [12]. The surface layers were sputtered off gradually, allowing XPS to perform on the inner layers. It showed that the Fe $2p_{3/2}$ peak was shifting to the lower binding energy side until the depth over 50 nm. The XPS graphs performed at the depth of 80 nm and 500 nm are shown in Fig. 4(b) and there is no peak shift between the two graphs, indicating that we were measuring the true binding energy of Fe in FeSe. In contrast to Fe, the binding energy of Se shifted very little with the depth, as shown in Fig. 4(c), indicating that oxygen has little effect on the Se valence.

It is apparent that the Fe $2p_{3/2}$ peak in Fig. 4(d) is not symmetric and composed of two peaks. After the deduction of background with the Shirley function, two peaks can be deconvoluted at 707.8 eV and 706.6 eV, respectively. The former was close to the value of Fe in the polarized ionic bonds, such as in $Na_3Fe(CN)_5NH_3$ [13], while the later had the typical value in the metallic bondings, such as in pure Fe metal [14]. For comparison, the XPS graph of a sintered powder sample is also shown in Fig. 4(d), which was performed after sputtering away a surface layer of 1.0 μm thick. Apparently, the ionic bonding contribution is more significant for the powder sample. Similar deconvolution gave the two binding energy peaks at 708.4 eV and 706.7 eV, respectively. The ratio of the two bondings, which was calculated by the areas under each of the deconvoluted peaks, was 1.56 and 1.94 for the films and sin-

tered powders, respectively, indicating a lower average Fe valence for thick films. In view of the fact that thick films were grown at high temperature in reduction atmosphere, lower Fe valence seems to be reasonable. The above results show that there probably exist two Fe valence states in FeSe. This is a consequence of the nonstoichiometric composition of the superconducting β-phase, whose formula is actually $FeSe_{1-x}$ ($x = 0.024–0.039$ [9]), implying that Fe is unlikely to have a single valence of 2+. The lower T_c observed in thick films may be related to their lower average Fe valence, because similar T_c reductions with the Fe valence state were also observed in $Fe_{1-x}Cu_xSe_{0.85}$ [6], whose T_c dropped constantly from 8 K to 2 K when the Fe valence was reduced from +1.81 ($x = 0$ sample) to +1.73 ($x = 0.02$ sample), and the superconductivity disappeared completely when the Fe valence was +1.66 ($x = 0.04$ sample) [6].

4. Conclusions

In conclusion, thick FeSe films were grown from high temperature solution with a quality similar to single crystal. However, the observed T_c was lower than the sintered powder samples. The Sn contamination from the flux was extremely low (<10 ppm) and its influence on T_c could be excluded. XRD did not find any notable structure distortion in the thick films except for a narrow peak width, confirming their better crystallinity. XPS revealed two Fe valence states in FeSe and the relative amount of the two bondings may have some correlation with the critical temperature. A lower average Fe valence may be responsible for the lower T_c observed in thick films.

Acknowledgements

This work was partially supported by the National Science Council of Taiwan under the grant number: NSC-96-2628-E-006-010-MY3 and by the National Cheng Kung University via Landmark Projects.

References

[1] I.I. Mazin, Nature 464 (2010) 183.
[2] F.C. Hsu, J.Y. Luo, K.W. Yeh, T.K. Chen, T.W. Huang, P.M. Wu, Y.C. Lee, Y.L. Huang, Y.Y. Chu, D.C. Yan, M.K. Wu, PNAS 105 (2008) 14262.
[3] M.D. Lumsden, A.D. Christianson, J. Phys.: Condens. Matter 22 (2010) 203203.
[4] K.W. Yeh, T.W. Huang, Y.L. Huang, T.K. Chen, F.C. Hsu, P.M. Wu, Y.C. Lee, Y.Y. Chu, C.L. Chen, J.Y. Luo, D.C. Yan, M.K. Wu, EPL 84 (2008) 37002.
[5] M.K. Wu, F.C. Hsu, K.W. Yeh, T.W. Huang, J.Y. Luo, M.J. Wang, H.H. Chang, T.K. Chen, S.M. Rao, B.H. Mok, C.L. Chen, Y.L. Huang, C.T. Ke, P.M. Wu, A.M. Chang, C.T. Wu, T.P. Perng, Physica C 469 (2009) 340.
[6] T.W. Huang, T.K. Chen, K.W. Yeh, C.T. Ke, C.L. Chen, Y.L. Huang, F.C. Hsu, M.K. Wu, P.M. Wu, M. Avdeev, A.J. Studer, arXiv:0907.4001.
[7] Y. Mizuguchi, F. Tomioka, S. Tsuda, T. Yamaguchi, Y. Takano, J. Phys. Soc. Jpn. 78 (2009) 074712.
[8] M. Yoshikazu, T. Fumiaki, T. Shunsuke, Y. Takahide, T. Yoshihiko, Appl. Phys. Lett. 93 (2008) 152505.
[9] P. Villars, A. Prince, H. Okamoto, Handbook of Ternary Alloy Phase Diagrams, vol. 8, ASM International, 1995, p. 10847.
[10] X. Qi, J.Y. Wang, C.J. Hung, J.C. Kuo, K. Yates, L. Cohen, J. Am. Ceram. Soc. 93 (2010) 3195.
[11] M.J. Wang, J.Y. Luo, T.W. Huang, H.H. Chang, T.K. Chen, F.C. Hsu, C.T. Wu, P.M. Wu, A.M. Chang, M.K. Wu, PRL 103 (2009) 117002.
[12] N.S. McIntyre, D.G. Zetaruk, Anal. Chem. 49 (1977) 1521.
[13] K.B. Yatsimirskii, V.V. Nemoshalenko, Y.P. Nazarenko, V.G. Aleshin, V.V. Hilinskaya, N.A. Tomashevsky, J. Electron. Spectrosc. Relat. Phenom. 10 (1977) 239.
[14] A. Lebugle, U. Axelsson, R. Nyholm, N. Martensson, Phys. Scr. 23 (1981) 825.